REVIEWS OF GEOPHYSICS VOL. 7, NOS. 1, 2 FEBRUARY-MAY 1969

Low-Frequency Waves in the Magnetosphere[1]

R. A. HELLIWELL

Radioscience Laboratory
Stanford University,
Stanford, California 94305

Abstract. In the magnetosphere are found low-frequency (100–100,000 Hz) electromagnetic waves generated externally by lightning and ground-based transmitters and internally by energetic charged particles. Dispersion and anisotropy characterize the medium, and both ducted and nonducted paths of propagation are found. Lightning-generated ducted 'whistlers,' observed on the ground, give information on the distribution of electrons and the latitudinal drift motions of ducts in the magnetosphere. Nonducted whistlers observed in satellites give information on electron and ion concentrations, the earth's magnetic field, and wave damping by energetic particles.

Noise generated in the magnetosphere (or ionosphere) includes steady noise, or hiss, and the structured forms known as discrete emissions. In the auroral zone, hiss is seen in close association with the aurora and over a frequency range of at least 4 kHz to several hundred kHz. It has been attributed tentatively to incoherent Cerenkov radiation from the incoming auroral particles. At middle latitudes, noise from the magnetosphere is mostly of the discrete type with associated hiss and appears to be limited to frequencies below the minimum gyrofrequency on the path of propagation. A related type of noise, called 'polar chorus,' appears at high latitudes below about 1500 Hz. Discrete emissions may occur spontaneously or be triggered by whistlers or man-made signals from the ground. The upper cutoff frequency is controlled by the minimum gyrofrequency on the path of propagation, indicating that the region of generation lies in the equatorial plane. Discrete emissions have been attributed to cyclotron resonance between whistler-mode waves and electrons. Emissions offer new possibilities for studying wave-particle interactions in the earth's magnetosphere and in other plasmas, both natural and man-made.

INTRODUCTION

In the magnetosphere, low-frequency (100–100,000 Hz) waves appear in a remarkable variety of forms. They may be introduced by lightning discharges and transmitters located below the ionosphere or be generated within the magnetosphere by wave-particle interactions. The propagation of waves in the magnetosphere is now relatively well understood. Certain phenomena, such as ducted nose whistlers, have already been applied to the quantitative study of the magnetosphere. Emissions generated within the magnetosphere are less well understood and constitute one of the outstanding problem areas in magneto-

[1] Invited review paper presented at the International Symposium on the Physics of the Magnetosphere, September 3–13, 1968, Washington, D. C.

spheric physics. VLF emissions offer possibilities as diagnostic tools for the study of energetic trapped radiation. They also offer a new approach to the study of plasma physics in an environment that is free of many of the restrictions of terrestrial laboratories.

Understanding of VLF waves in the magnetosphere began for all practical purposes with Storey's classic paper on whistlers [*Storey*, 1953]. Use of whistlers to study the electron distribution in the magnetosphere became well established during the IGY [*Helliwell*, 1965]. Subsequent growth of research on whistlers and related phenomena has closely paralleled the growth of space research itself. Indeed, some of the most important results pertaining to VLF waves in the magnetosphere are the direct result of satellite experimentation. It should be emphasized that satellite and ground observations are complementary in nature and that many results of the greatest importance have required both kinds of measurements.

It is the purpose of this paper to review the propagation and emission of waves in the magnetosphere at frequencies below the local electron gyrofrequency in the range 100 Hz to 100 kHz. Owing to space limitations, this review cannot be comprehensive. Hence, it emphasizes basic concepts and their applications and tries to focus attention on the more important unsolved problems.

PROPAGATION

In discussing propagation of low-frequency waves in the magnetosphere, it is convenient to consider separately 'ducted' and 'nonducted' propagation. The term 'ducted' refers to waves that are confined to field-aligned paths in the magnetosphere. These paths are thought to consist of field-aligned irregularities of ionization that trap waves whose wave normals lie within a certain angle with respect to the earth's magnetic field. Ducted propagation is important because it is almost the only means by which many VLF-wave phenomena in the magnetosphere can be detected on the ground. The term 'nonducted' on the other hand refers to waves that are not trapped by field-aligned irregularities. Nonducted propagation is distinguished by the fact that the ray paths deviate from the direction of the earth's magnetic field, and the wave normal may show large variations in direction with respect to the earth's magnetic field. With few exceptions, nonducted propagation has been observed only by rockets or satellites located within the ionosphere or magnetosphere. Most ducted propagation from the ground is observed to occur within the plasmasphere, although occasionally ducted whistlers are observed out to $L = 9$ on the dayside of the earth.

Ducted propagation. The characteristics of ducted propagation are illustrated by the phenomenon of echoing whistlers, depicted in Figure 1. A single duct is shown, and the spectra to be expected at points A, B, C, and D are sketched in the right-hand part of the diagram. The signal source is a lightning flash located near point A. The receiver at A observes a strong impulse followed by a succession of whistlers spaced uniformly in time in the ratios 2, 4, 6, etc. At the conjugate point D, the impulse is usually very weak or undetectable and is followed by 1-hop, 3-hop, 5-hop whistlers, etc. The delays in such conjugate echoing trains are generally exact integer multiples of the 1-hop delay. This fact is one of sev-

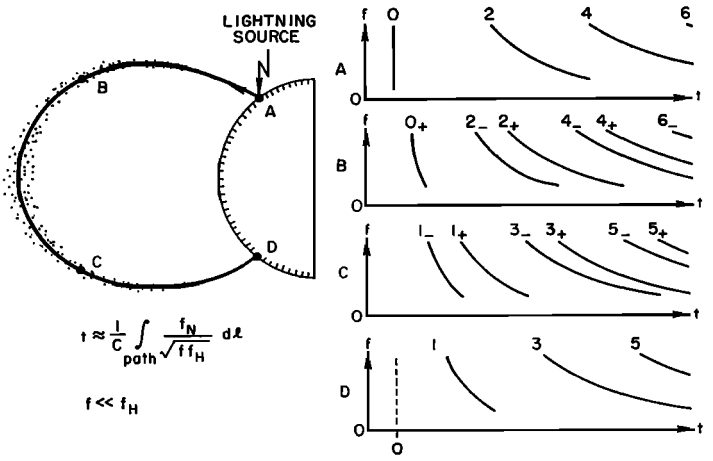

Fig. 1. Echoing ducted whistlers as observed on the ground at points A and D and in satellites at points B and C. The lightning source is located at point A, and the Eckersley approximation is used to sketch the spectra. The vertical dashed line in the lowest spectrogram represents the attenuated sferic arriving at D via the earth-ionosphere waveguide.

eral indicating that the path of propagation must be fixed in the magnetosphere. Satellites, located within the duct at points B and C, observe fractional-hop whistlers, as shown in Figure 1. If the lightning flash were located at point D, then the order of the spectra would be reversed. A sufficiently strong impulse would excite both ends of the path almost simultaneously, giving a superposition, called 'hybrid,' of the two types of spectra at each station.

Although only a single duct has been pictured in Figure 1, it is common for several ducts to be observed simultaneously. If the latitude of observation is sufficiently high, the whistler nose, or frequency of minimum time delay, can often be observed. An example of two 1-hop nose whistlers excited by a single impulse is shown in Figure 2. The nose frequency f_n is closely related to the minimum gyrofrequency along the path, as indicated in Figure 2. Assuming a dipole field, the path latitude can, of course, be found from the minimum gyrofrequency. With this information and the time delay at the nose, it is possible to determine the scale factor for the electron concentration, assuming a form for $f_N(l)$ in the time delay integral shown in the figure. On the other hand, if the base-level plasma frequency is known, say, from topside soundings, a parameter giving the scale height can be found. From this type of information it has been found that the plasmasphere can be described approximately by a diffusive equilibrium model [*Angerami and Carpenter,* 1966].

An outstanding feature of many nose whistlers is a sharp upper cutoff. Detailed analysis has shown that this cutoff occurs very close to half the minimum gyrofrequency [*Carpenter,* 1968*a*], a value predicted in *Smith's* [1961] theory of duct trapping. The close agreement between the prediction and the measure-

ment in this case gives strong support to the theory of whistler trapping by field-aligned enhancements of ionization.

Occasionally a satellite (e.g., OGO 1) will observe a sequence of nose whistlers in which the change in nose frequency is discontinuous, indicating the presence of a set of ducts [*Smith and Angerami*, 1968]. Furthermore, it is sometimes possible to observe the leakage signals that escape from the duct when they reach the point where the frequency is equal to one-half the gyrofrequency (J. J. Angerami, private communication). A sketch of a spectrogram illustrating this effect and the corresponding path is shown in Figure 2.

Trains of nose whistlers generally show a smooth decrease in nose frequency with nose delay. Frequently, however, a discontinuity occurs in the train at a particular frequency, below which may be seen one or more nose whistlers with greatly reduced time delays. An example of such a shifted trace (called a 'knee' trace) is shown in Figure 3; it is the result of propagation through a low-density plasma outside the 'knee' or plasmapause. By using records of this type, it has been possible to determine the location of the plasmapause and the magnitude of the density change. Decreases by factors of 10 to 100 may occur in a space of less than 1 R_E. Use of this technique throughout the day gives a map of the location of the plasmapause [*Carpenter*, 1966] as a function of local time, as illustrated in Figure 3. The possibility of 'sounding' the plasmapause and the magnetopause at frequencies above the plasma frequency is also suggested in the figure.

At ground stations, such as Eights, Antarctica, where the rate of whistler occurrence is very high, it is possible to follow the change with time of the lati-

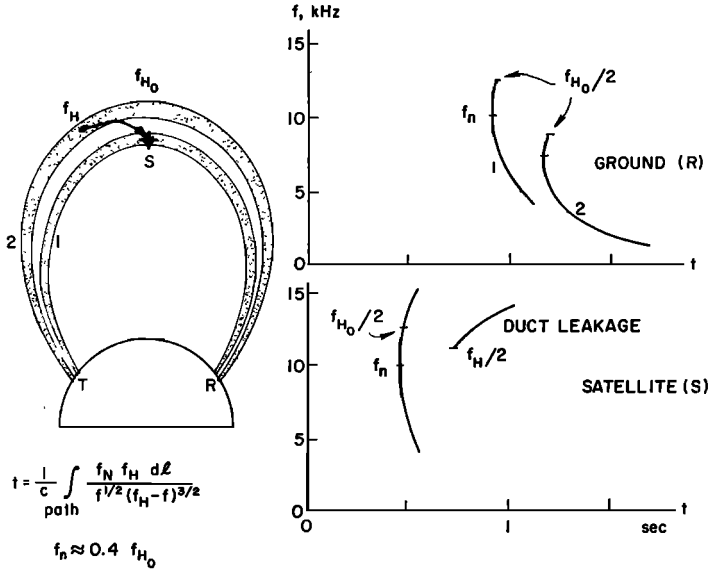

Fig. 2. Multipath ducted nose whistlers observed on ground; leakage from ducts observed on satellite for $f > f_H/2$. Nose frequency f_n gives path latitude; nose delay t_n gives electron concentration. f_H = electron gyrofrequency, f_N = electron plasma frequency, dl = element of path.

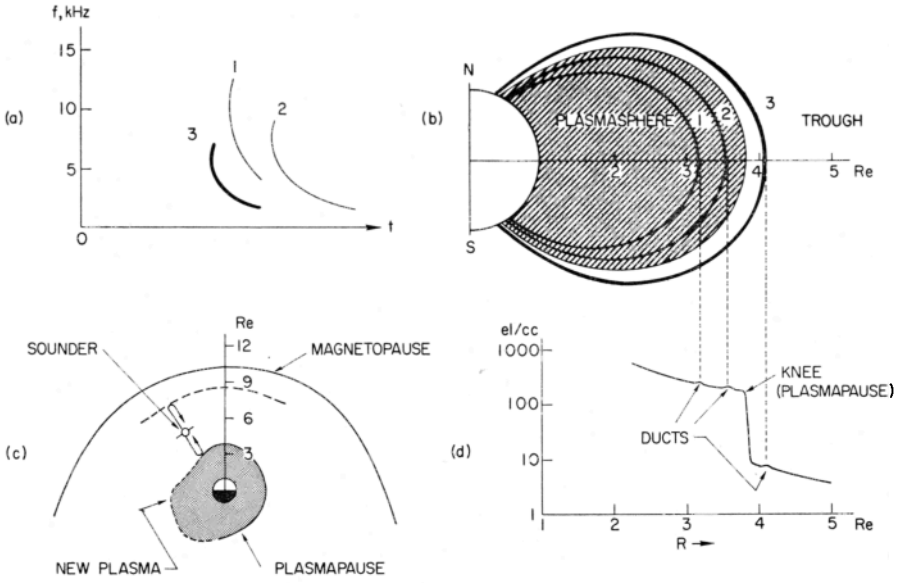

Fig. 3. (*a*) Nose whistler train, with knee trace; (*b*) meridional plane showing whistler ducts; (*c*) boundary of plasmasphere deduced from knee trace, possible detection of plasmapause and magnetopause by low-frequency sounder located in trough; (*d*) equatorial profile of electron density deduced from (*a*).

tudes of the whistler ducts [*Carpenter*, 1968*b*]. This change is detected by the progressive change in the nose frequencies of a set of whistler traces. Inward and outward drifts of ducts of up to 0.4 R_E/hour have been found, and these drifts are interpreted in terms of an east-west electric field ($\sim$ 0.5 mv/m) in the magnetosphere causing latitudinal movements of the plasma. New information on the circulation pattern of the thermal plasma is being obtained by this method.

Nonducted propagation. In nonducted propagation the wave energy is not guided along the earth's field by a field-aligned irregularity in electron density. Nonducted propagation may occur not only in the absence of ducts but also when the wave normal angle exceeds the trapping angle of a duct or when the point of excitation lies outside the duct. In the absence of duct effects, the usual distribution of refractive index is such as to cause the wave normals to depart gradually from the direction of the earth's field, as shown in Figure 4. Upon

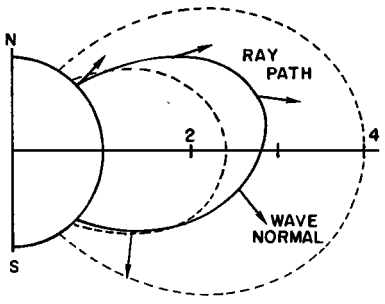

Fig. 4. Typical nonducted ray path (solid line) of signal on 15.5 kHz from ground source located at 45° magnetic latitude for a constant density model [after *Yabroff*, 1961]. Wave normal direction, shown by arrows, gradually departs from direction of magnetic field. Dipole field lines are shown dashed.

reaching the opposite hemisphere, nonducted waves have such large wave normal angles that they cannot propagate across the lower boundary of the ionosphere and hence are not observed on the ground.

If the frequency is sufficiently low, the whistler may be reflected in the vicinity of the lower hybrid resonance (LHR) frequency and hence never reach the lower boundary of the ionosphere. An example of a nonducted magnetospherically reflected (MR) whistler observed with OGO 1 is shown in Figure 5. The mechanism of reflection in the vicinity of lower hybrid resonance is illustrated by the diagrams of Figure 6, which show the ray paths for one frequency. The essential feature of this process is the closing of the refractive index surface at the lower hybrid resonance frequency f_L. As the diagram shows, using Snell's law construction, the ray path swings around and reverses its direction, as the wave propagates into the region of the lower hybrid resonance. This process of reflection is repeated each time the wave approaches the LHR region. As the satellite moves across the equator, the relative spacing between echoes changes in a predictable way. These spacings therefore give information on the location of the magnetic equator as well as a measure of the electron density. The separation between the third and fourth component of an MR whistler provides information on the ion composition at 1000 km (B. Edgar, private communication), whereas enhancement of the intensity of the echoes together with their cutoff frequencies gives information on wave-particle interactions [*Thorne*, 1968].

At lower altitudes and occasionally on the ground the 'subprotonospheric' (SP) whistler can be seen [*Carpenter et al.*, 1964]. This phenomenon depends on the presence of ions and basically consists of whistlers that echo back and

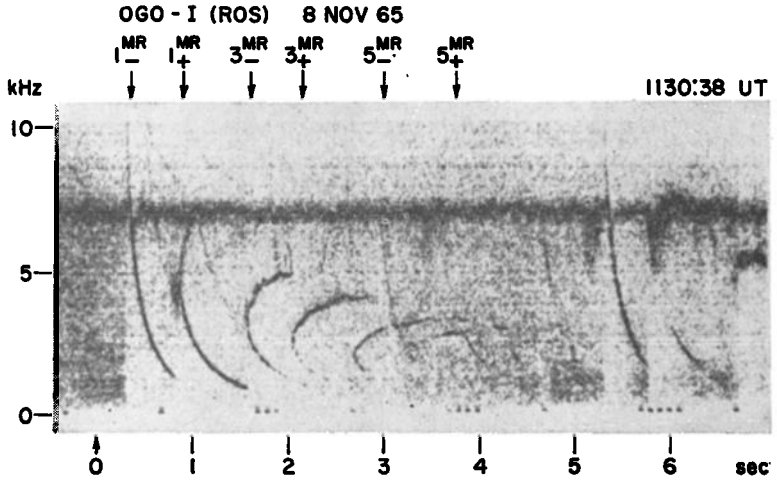

Fig. 5. Magnetospherically reflected (MR) whistler [after *Smith and Angerami*, 1968]. Geomagnetic latitude = 5.9°S, L = 2.4, altitude = 8749 km, local time = 0520. Dark trace at 7 kHz is produced by a voltage-controlled oscillator used to indicate relative amplitude. Background noise is weakened by strong whistler components through the action of the instantaneous automatic gain control of the receiver.

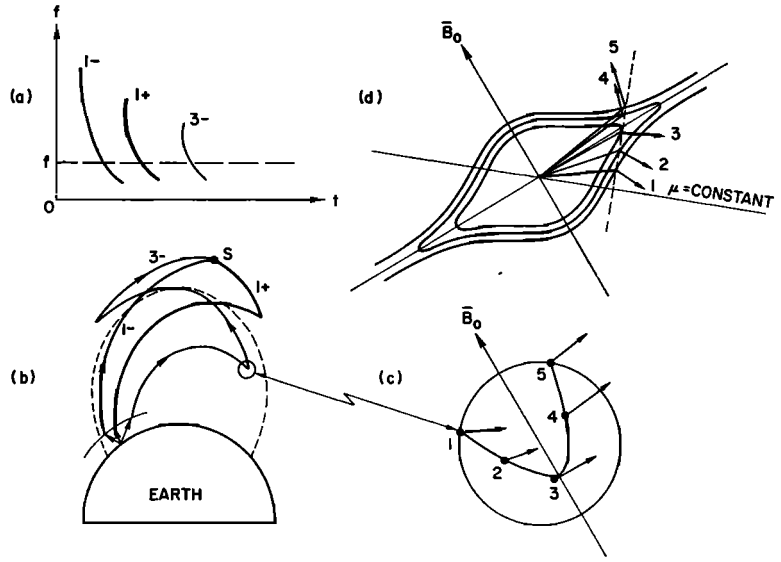

Fig. 6. Interpretation of MR whistlers: (*a*) Idealized spectrum observed in satellite; (*b*) ray paths to satellites at frequency f; (*c*) enlarged view of 'turn-around' region, showing wave normal directions; (*d*) refractive index surfaces in vicinity of 'turn-around,' showing mechanism of reflection. Dashed line is perpendicular to surfaces of constant refractive index.

forth between the lower edge of the ionosphere and a reflection level near 1000 km [*Smith*, 1964; *Kimura*, 1966].

Related to the SP whistlers are the so-called ion whistlers, including the proton [*Gurnett et al.*, 1965] and helium [*Barrington et al.*, 1966] whistlers and the recently identified ion-cutoff whistler [*Muzzio*, 1968]. Each of these whistlers depends on the presence of multiple ions in the magnetosphere. An electron whistler traveling upward toward the satellite can be converted to the left-hand polarized mode at the crossover frequency f_x, as shown in Figure 7. As the frequency of the left-hand circularly polarized wave approaches the local proton gyrofrequency, the group delay increases, and the trace asymptotically approaches the local proton gyrofrequency F_H. The proton whistler separates from the electron whistler at the crossover frequency that measures the relative concentration of protons. The cutoff time of the ion whistler is a measure of the ion temperature of the region.

The ion cutoff whistler, illustrated in Figure 7, propagates down from the magnetosphere and is reflected in the vicinity of the cutoff frequency for the left-hand mode. It too provides information on the concentration of protons. The same reflection phenomenon may be the cause of the lower cutoff in emission spectra observed at altitudes below several hundred kilometers [*Guthart et al.*, 1968; *Gurnett and Burns*, 1968].

Another propagation phenomenon of interest is the so-called LHR whistler, which shows enhanced dispersion in the vicinity of the lower hybrid resonance.

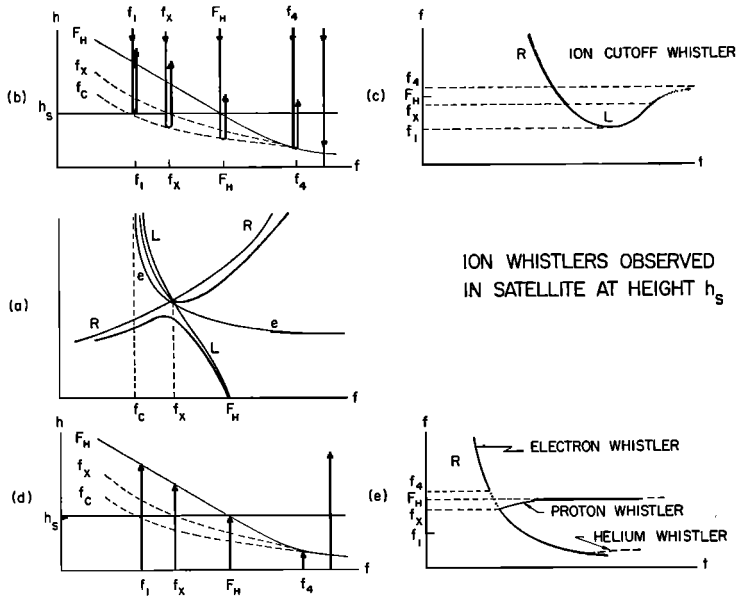

Fig. 7. Ion whistlers observed on a satellite: (*a*) Phase velocity versus frequency at satellite when 2 ions are present; (*b*) Reflection heights and polarization changes of rays incident from *above*; (*c*) Spectrum of *ion cutoff whistler* produced by paths sketched in (*b*); (*d*) Reflection heights and polarization changes of rays incident from below; (*e*) Spectrum of proton resonance whistler produced by paths sketched in (*d*); the helium whistler, shown dashed, requiring one more heavier ion than assumed in (*a*).

It is often seen in close association with a noise band having a sharp lower cutoff at the LHR, and it may appear to trigger hiss in the LHR band [*Barrington*, 1968]. Although it appears that the LHR whistler is related to dispersion near the LHR, the detailed mechanism has not yet been established.

In addition to the dispersion phenomena already described, the propagation of man-made signals from the ground to satellites is of interest [*Heyborne*, 1966]. These signals have been observed at many frequencies between 6 and 95 kHz. Generally the signal strength follows expected laws, but rapid 1-sec deep fading of unexplained origin is often observed. At the higher frequencies (80 kHz), the cutoff is often as high as 0.9 or 0.95 of the local gyrofrequency (N. Dunckel, private communication) and may be evidence of Landau damping. At latitudes above the knee, roughly 60°, propagation of VLF waves from the ground to satellites is often severely attenuated; in the same region a noise resembling hiss is often observed [*Heyborne*, 1966]. Although the cause of this latitudinal cutoff is not known, *D*-region absorption enhanced by particle precipitation is a possibility.

EMISSION OF WAVES

In the previous section we considered the waves that originate in sources below the lower edge of the ionosphere. In addition there are other waves, called

'emissions,' that appear to have their source within the magnetosphere. One of the problems in this field of study is to separate propagation from source effects. Sometimes a propagation effect can be identified by associating the phenomenon in question with the impulse from a lightning flash; however, identification of the source itself is sometimes not sufficient to permit the separation of emission and propagation effects. The reason is that many emissions are in fact triggered by whistler-mode signals from the ground. Thus, in the last analysis, it is necessary to have a comprehensive understanding of propagation in the medium and the phenomena resulting from propagation effects. The division between emission and propagation effects is becoming increasingly better understood, and we can now identify many of the emission forms. The basis for classifying emissions is partly their spectral characteristics and partly their regions of occurrence. In the following paragraphs we shall consider the prominent forms of emissions from the magnetosphere.

Emission phenomena. One of the simplest types of emissions in terms of its spectral characteristics is the so-called auroral hiss seen on the ground, which constitutes the first major class of VLF emissions. This noise is observed in the auroral zone in close association with visible aurora [*Morozumi,* 1965]. Its spectrum resembles band-limited white noise, which may or may not show rapid fluctuations with time. The spectrum tends to peak in the vicinity of 10–20 kHz with a low frequency cutoff at about 4 kHz and an upper frequency cutoff as high as several hundred kHz. Auroral hiss is not associated with whistlers and seldom shows any evidence of whistler-mode dispersion. It is important to distinguish auroral hiss from the so-called midlatitude hiss, which is closely associated with discrete emissions.

Auroral-zone noise is also seen in satellites, but it has been singularly difficult to associate the satellite observations directly with events on the ground [*Gurnett,* 1966]. Satellite-observed hiss is closely associated with fluxes of soft electrons (3–4 kev).

Some idea of the present state of knowledge of auroral zone VLF noise can be obtained from Figure 8 in which the spectra typically observed in a hiss burst at Byrd are shown together with spectra observed in the OGO 2 satellite. The geographical distribution of hiss bursts recorded by Injun 3 with intensities exceeding those indicated in Figure 8*b* is shown in Figure 8*a*. It is seen that the hiss observed in Injun 3 tends to be concentrated mainly in the noon-to-midnight time sector.

Another type of noise detected by satellites and associated with the lower hybrid resonance frequency [*Barrington,* 1968] is observed at both high and low latitudes but has never been identified on the ground. Its low frequency cutoff is fairly steady at middle latitudes but fluctuates widely at polar latitudes. Other differences between 'midlatitude' and 'polar' LHR noise are found in their diurnal and seasonal variations.

The propagation cutoff effects noted in connection with the lower hybrid resonance may explain some of the observed noise bands near the LHR [*Storey and Cerisier,* 1968]. Thus, VLF emissions propagating downward from the magnetosphere will tend to be cut off near the LHR frequency and hence appear to be

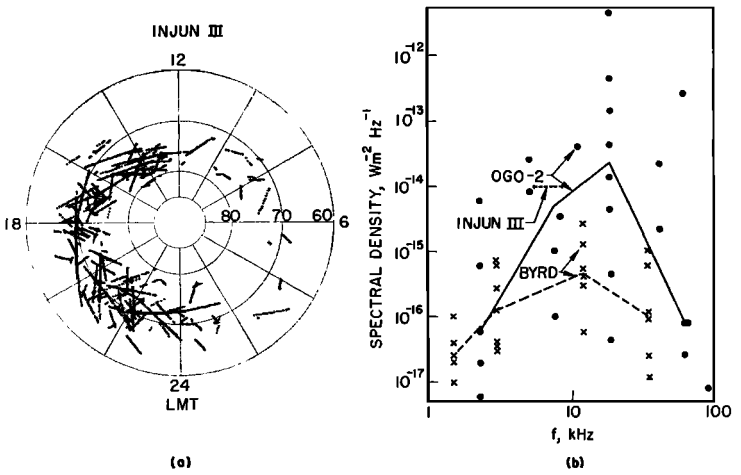

Fig. 8. Auroral hiss: (*a*) Geographical distribution (in local mean time and invariant latitude) of hiss recorded by Injun 3 between 5.5 and 8.8 kHz [after *Gurnett,* 1966]; (*b*) Spectrum of hiss burst observed at Byrd, August 3, 1966, and spectrum of hiss observed on multiple passes of OGO 2 through auroral zone, November 12–23, 1965 [*Jørgensen,* 1968].

associated with the local LHR. On the other hand, as noted in the discussion of nonducted propagation, both long and short whistlers are observed to produce enhancements of LHR noise. This implies that the effects are local in origin and, in fact, might be due to the dispersion of waves introduced from outside the LHR region.

The second major class of VLF emissions shows marked structure in its spectral characteristics. This class includes the well-known discrete emissions, such as chorus and associated hiss, observed at middle latitudes and the polar chorus observed in the polar regions. The distinguishing characteristic of this class of emissions is the presence of well-defined short-duration tones with either a rising or falling characteristic or a combination thereof. These discrete elements often appear in a background of steady hiss or at the upper edge of a hiss band. The discrete elements may be repeated with slightly different forms many times per second, resembling in sound the waking of birds in the early morning. From this analogy came the descriptive term, 'dawn chorus,' which is usually simply shortened to 'chorus.' An example of chorus recorded on the ground is shown in Figure 9*a*.

Satellites traveling within the regions of closed field lines also observe discrete emissions and associated hiss. Unlike ground observatories, satellites are not restricted to observing signals propagating in ducts. In fact, much of the noise observed in high altitude satellites is of the nonducted variety. Thus, the satellite data relate to a different regime of emissions and propagation.

An example of discrete emissions recorded in OGO 1 (W. Burtis, private communication) is shown in Figure 9*b*: note that the individual element of the ground and satellite spectra is rather similar. However, one very important difference is observed. As a satellite moves through space, the upper cutoff frequency

of these emissions changes with L value. It is controlled not by the local gyrofrequency at the satellite but rather by the minimum gyrofrequency on the field line passing through the satellite. Equatorial control of the frequency of generation implies that the generator must lie close to the equatorial plane. If the emission source were located elsewhere, the cutoff frequency should not always be connected with the minimum gyrofrequency along the path, since the satellite would frequently intercept such emissions before they passed the equatorial plane.

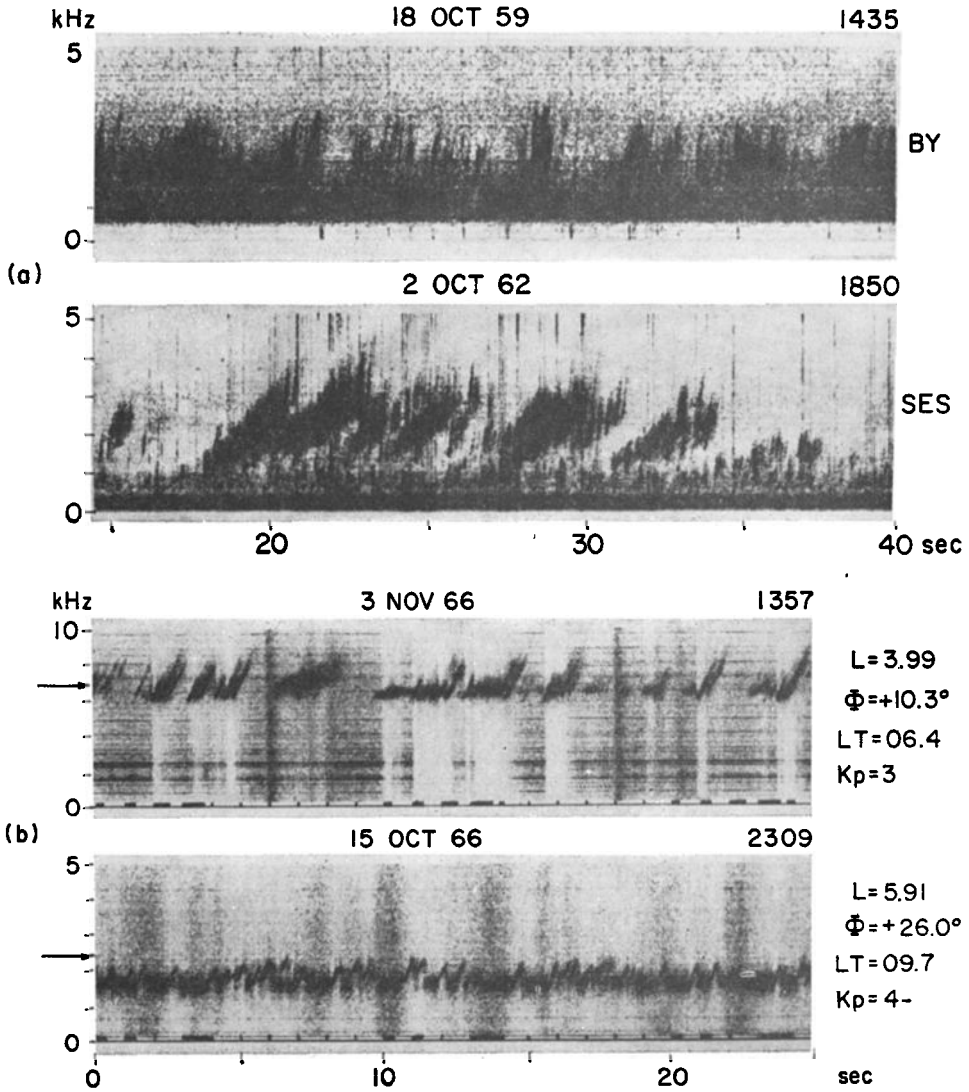

Fig. 9. Discrete emissions: (*a*) Ducted discrete emissions of the rising type ('chorus') recorded on the ground [*Helliwell*, 1965; see Figure 7-31]; (*b*) Nonducted discrete emissions recorded on OGO 1; arrows on frequency scale indicate the minimum gyrofrequency on field line through the satellite.

In the polar regions a mixture of chorus and hiss called 'polar chorus' is observed mainly in the range 400–1500 Hz. This noise tends to be a daytime phenomenon and is clearly not connected with the auroral hiss described previously. Its origin has in the past been attributed to cyclotron radiation by protons in the ionosphere. However, inspection of the distribution of discrete emissions observed by the OGO 1 satellite shows that, if the noise generated in the equatorial plane in this frequency range is mapped to the surface of the earth, its occurrence is similar to that of the polar chorus (N. Dunckel, private communication). Furthermore, the spectral properties of the OGO 1 noise resemble those observed by ground stations in the polar regions. It appears possible, therefore, that the polar chorus is simply an emission from the equatorial plane that has propagated in a duct to the polar regions.

A further distinguishing property of discrete emissions is their tendency to be triggered by other signals. Although discrete emissions often occur spontaneously, as in chorus, they are sometimes seen only in association with a strong triggering signal. Whistlers themselves may trigger discrete emissions at the whistler upper cutoff frequency ($f_{H0}/2$) or at various lower frequencies. An example of triggering at the upper cutoff on several paths is shown in the lower panel of Figure 10*a* [*Carpenter*, 1968*a*]. Also shown in Figure 10*a* (upper panel) is a train of nose whistlers showing very little triggering. Often bursts of discrete emissions lasting 10 or 20 sec are observed to follow a strong whistler. Even more remarkable is the fact that an emission can often be triggered by the whistler-mode echo of a previous emission. This process may be repeated many times giving trains of periodic emissions that may last for minutes or even hours. The period between such emissions is exactly the period of 2-hop whistler transmission at the triggering frequency. Often several sets of periodic emissions having different phases can exist simultaneously in the same duct.

Another type of triggered emission or interaction is observed in satellites in connection with MR whistlers. The tops of these whistlers are often accompanied by enhancement or broadening of the whistler trace. These 'emissions' are generally different in form from those observed on the ground and suggest that a different mechanism may be involved. Since the MR whistler is characterized by a large wave normal angle, it is possible that these emissions are connected with longitudinal resonance as suggested by *Thorne* [1968].

Triggering of discrete VLF emissions is also observed in connection with transmission from ground-based VLF transmitters of both high power (10^6 watts) [*Helliwell*, 1965] and low power (100 watts) [*Kimura*, 1968]. The likelihood of triggering is far greater with Morse-code dashes (approximately 150 msec) than with Morse dots (approximately 50 msec) as illustrated in Figure 10*b*. Furthermore the onset of the triggered emission is delayed with respect to the onset of the triggering signal by times of the order of 100 msec. These two facts taken together suggest that the duration of the triggering signal must exceed the triggering delay to produce an emission. Although triggering by whistlers and man-made signals can occur over a considerable range of frequencies, it has been found that triggering is most common when the triggering frequency is equal to one-half the minimum gyrofrequency on the path. This tendency has even been

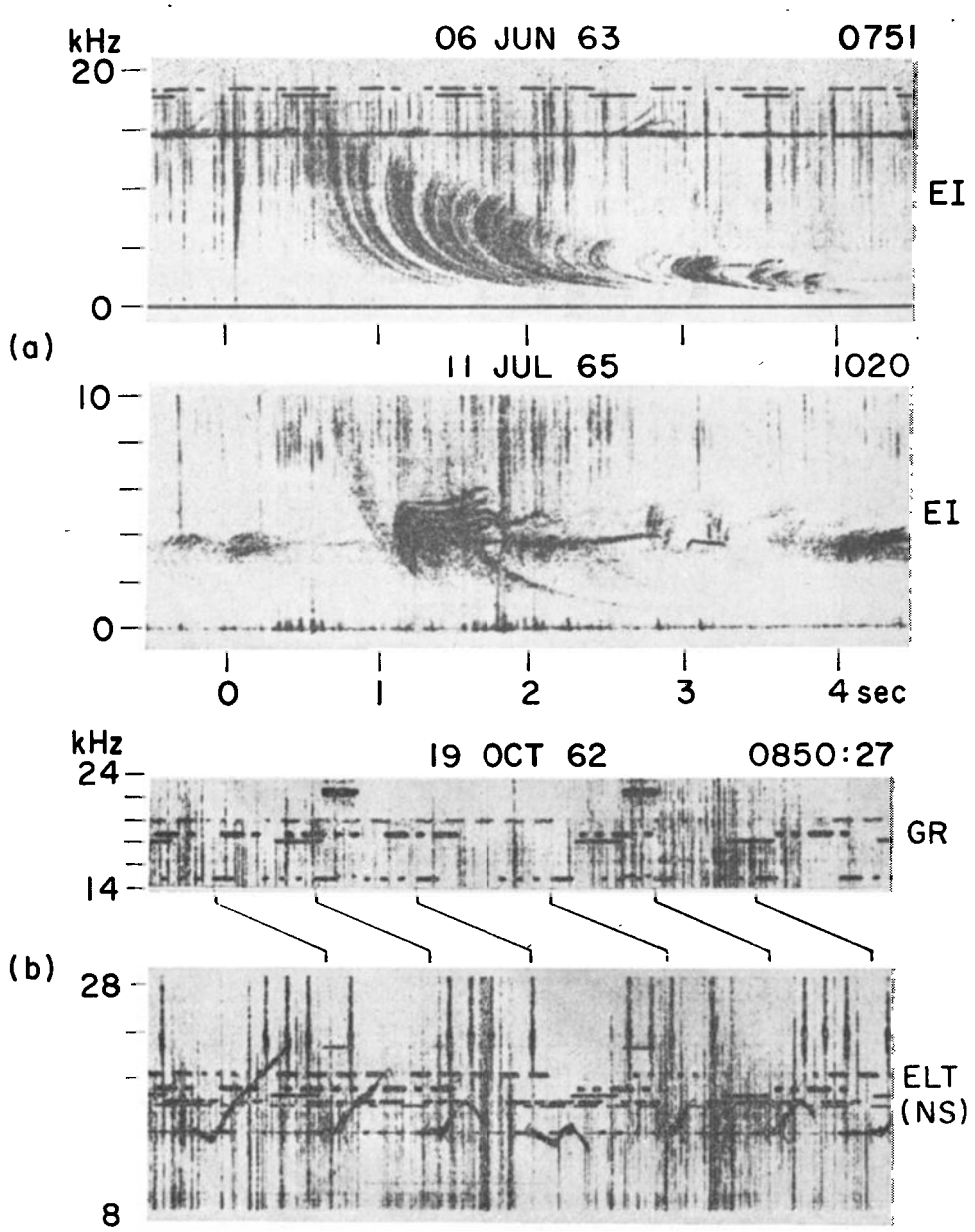

Fig. 10. Triggered emissions: (*a*) Upper panel shows multipath nose whistler and rising tones triggered by NAA at 14.7 kHz; lower panel shows discrete emissions triggered by nose whistlers at their upper cutoff frequencies ($f_{H0}/2$), Eights Station, June 6, 1963, 0751 UT; (*b*) Artificially stimulated emissions (ASE's) from the Morse-code dashes transmitted by station NAA [*Helliwell*, 1965; see Figure 7-65*a*, *b*]; lines connect the direct wave observed near the transmitter with its whistler-mode echo observed near the conjugate point.

found in connection with drifting ducts [*Carpenter*, 1968*b*]. In this case the triggering was observed to increase markedly when the duct drifted past the latitude at which the transmitter was exactly one-half the minimum gyrofrequency.

From the facts regarding triggering of emissions at half the minimum gyrofrequency, we can draw inferences regarding the region and mechanism of generation. First, we note that the cutoff of whistlers at half the gyrofrequency is a duct trapping phenomenon. To explain the triggering of emissions at half the minimum gyrofrequency by whistlers, one might suppose that the emission is initiated by the sudden termination of the whistler itself. If this were true, then the location of the triggering region could be anywhere on the line of force. However, if triggering by the termination of the triggering signal were the main effect, then artificially stimulated emissions (ASE) should be observed over a range of frequencies comparable to the range over which triggering by nose whistlers has been observed. However, the ASE's are seen to be triggered predominately at half the minimum gyrofrequency as well. Furthermore ASE's often begin *before* the termination of the triggering signal. Thus it appears that the sudden termination of the signal has little to do with triggering. Examining the parameters of the magnetosphere, we find that half the minimum gyrofrequency is characteristic only of the top of the path, that is, the magnetic equator. We conclude therefore that the emission must be generated near the equator.

Having established the location of the generation region, we must explain the particular value ($f_{H0}/2$) of the triggering frequency. If we examine the condition for trapping in a duct, we find that, at frequencies greater than one-half the gyrofrequency, the waves are no longer trapped in an enhancement of ionization. Thus, we might be tempted to argue that the failure of trapping produces a sharp cutoff in the signal, which in turn produces triggering. However, we have already shown that the termination of the triggering signal is not the primary cause of emissions. The basic cause of the failure of trapping in an enhancement of ionization is simply the change in the shape of the refractive index surface from concave to convex. This change occurs whether a duct is present or not and hence applies to nonducted signals as well as ducted signals. Thus, it appears that we can eliminate the duct as an important factor in determining the frequency of triggering.

We are now left with only the change in the shape of the refractive index surface at one-half the gyrofrequency. One property of this change is the reversal of the sense relation between wave normal and wave direction. However, since we are dealing with a uniaxial medium, it would appear that there can be no fundamental difference between these two situations with respect to the point properties of the wave. Now we are left only with the fact that at half the gyrofrequency the rate of change of curvature of the surface is zero for zero wave normal angle. At this frequency maximum ray focusing occurs. This effect should enhance the feedback between waves and particles as envisioned in the drifting cyclotron oscillator mechanism to be described below.

Emission mechanisms. Quantitative explanations of magnetospheric emissions are largely lacking. However, it is probable that the wave energy is provided by the relatively numerous nonrelativistic charged particles that resonate with

whistler-mode waves. The two resonances appropriate to this problem are the longitudinal (or Cerenkov) resonance and the transverse (or cyclotron) resonance. The resonance conditions are illustrated in Figure 11*a*.

As Figure 11*a* shows, the particle velocity for longitudinal resonance depends only on the phase velocity of the wave. Since the phase velocity shows relatively small variations with altitude, longitudinal resonance should be effective at all altitudes. In its simplest form this resonance gives rise to incoherent Cerenkov radiation, which until recently had been thought insufficient in strength to explain the observed radiation. Although incoherent Cerenkov radiation appears to be inadequate to account for observations of emissions at middle latitudes, recent research indicates that it may be sufficient to explain auroral hiss. Using satellite observations of the fluxes of low-energy electrons along the lines of force terminating in the auroral zone and using a realistic model of the region of generation, *Jørgensen* [1968] has found that the total power generated in the magnetosphere by incoherent Cerenkov radiation is comparable to the observed power in auroral hiss as shown in Figure 8. Electron energies involved in this calculation are of the order 1 to 10 kev.

Increased power can be obtained through the longitudinal resonance when conditions exist for a wave-particle instability. By postulating a humpy spectrum in the distribution of electrons, *Thorne* [1968] was able to explain both the cutoff and apparent growth features of MR whistlers. In addition, the emissions frequently seen in association with MR whistler traces are explained as the result of the Landau instability involving electrons in the 1- to 10-kev range.

Incoherent cyclotron radiation is likewise not sufficient to explain midlatitude VLF emission intensities [*Liemohn*, 1965]. However, processes have been identified in which small signals may grow at the cyclotron resonance, thereby increasing the intensity of the radiation [*Brice*, 1964; *Kimura*, 1967]. From the resonance condition given in Figure 11*a*, note that the cyclotron radiation and the

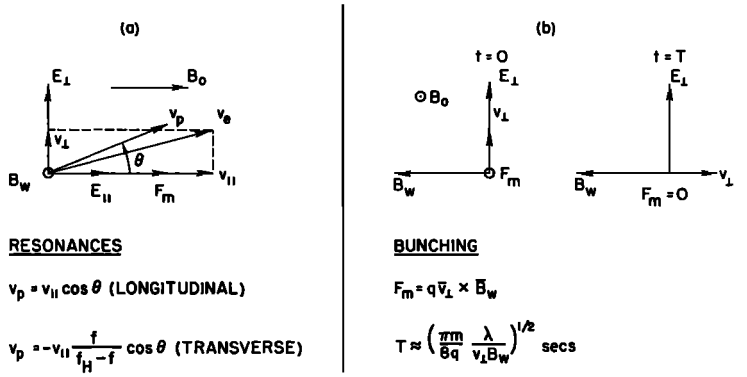

Fig. 11. (*a*) Wave-particle resonances: v_p = wave velocity, $v_\parallel$ = electron streaming velocity, f_H = electron gyrofrequency, B_0 = earth's magnetic field, B_w = wave's magnetic field, and E = wave's electric field; (*b*) Magnetic bunching: F_m = longitudinal bunching force, q = electron charge, m = electron mass, and λ = wavelength.

resonant electrons travel in opposite directions. This means that the output radiation can affect the incoming electrons thus providing the feedback needed to sustain an oscillation for an indefinite length of time at a fixed location. In the longitudinal resonance, on the other hand, the emitting region moves with the particles; hence, the duration of a coherent wave train must be limited to the travel time (<3 sec) over a field line path. However, much longer wave trains (>30 sec) have been observed, making this mechanism unacceptable.

An additional fact favoring cyclotron resonance as the basic cause of discrete emissions is the variation in particle energy requirement with gyrofrequency. As Figure 11*a* shows, the parallel velocity required for resonance depends upon the difference between the frequency of the wave and the electron gyrofrequency. At points far removed from the equator, generation at one-half the minimum gyrofrequency would take place at relatively large local gyrofrequencies, and hence the resonant parallel velocity of the electrons would increase, thus reducing the number of particles available. We conclude therefore that the cyclotron resonance interaction will be optimum in the vicinity of the equatorial plane as required by the observational evidence.

Having identified cyclotron resonance as the most likely source of radiation of discrete emissions, we now examine the particular characteristics of the radiation that must be explained by a detailed mechanism. The four outstanding features that must be explained by an acceptable theory are summarized and sketched in Figure 12. From the narrow bandwidth and the wide variation in center frequency, we deduce that the oscillation cannot be related to particular narrow peaks in the energy distribution of electrons. The continuous susceptibility of the magnetosphere to triggering, as mentioned earlier, eliminates the possibility that transient fluctuations in the distribution of resonant electrons could play an important role. Hence, we must look for a mechanism that is, to the first order, independent of the details of the distribution of energetic particles. The relative constancy of the amplitude of emissions indicates that the interaction process is self-limiting and therefore that small signal theories may not be usable. Furthermore, the 100-msec triggering delay and the predominance of triggering by dashes rather than by dots suggest that the growth process is nonlinear. It is especially remarkable that the center frequency of a narrow band emission can change by as much as a factor of 2 with little change in the average amplitude of the oscillations.

On the basis of the facts reviewed above, a phenomenological theory has been developed to explain the observed features of discrete VLF emissions [*Helliwell*, 1967]. The mechanism is based on magnetic phase bunching of the resonant electrons by the circularly polarized whistler-mode wave [*Brice*, 1963]. The mechanism of bunching is indicated in Figure 11*b*, in which the force relations are diagrammed at two different times, $t = 0$ and $t = T$. The interaction is viewed from the position of the resonant electrons whose unperturbed phase is constant with respect to the transverse components of the E and H fields of the wave. In Figure 11*b*, at $t = 0$, the transverse velocity of the resonant electron is shown at right angles to the magnetic field of the wave, so that the drift force F_m has its maximum value. As the resonant electron moves in response to this force

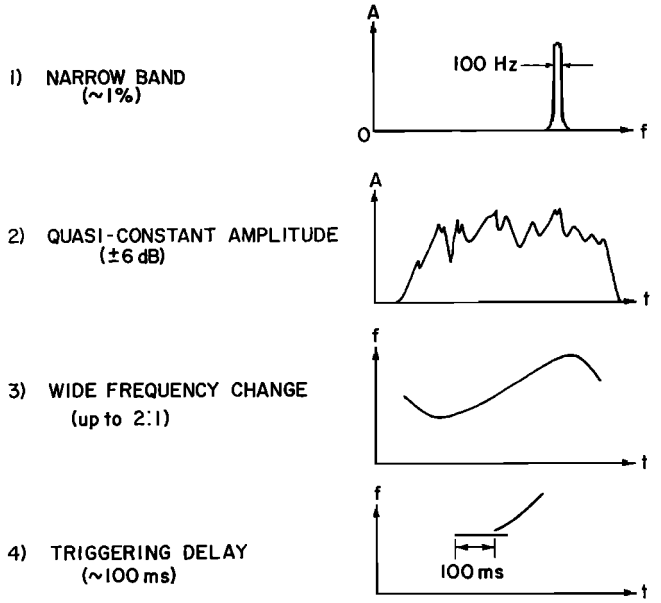

Fig. 12. Properties of discrete emissions.

its phase angle with respect to B_w decreases, eventually reversing the sign and thus causing the drift force to reverse. Since this force varies sinusoidally with displacement, it is clear that the resulting motion will be oscillatory. In fact it is identical to that of a simple pendulum. Thus, regardless where the electron finds itself initially, it will arrive at its stable point in approximately one-quarter of the pendulum period, denoted by T. This is called the bunching time and is seen to depend on the mass and charge of the electron, the wavelength of the excited radiation, the perpendicular velocity of the electron, and the wave magnetic field.

If now we consider a random set of electrons having all possible phase angles with respect to B_w, then it is clear that the perpendicular velocities will tend to line up in the wave's frame of reference at time T. At this time the vector sum of all the transverse currents carried by the individual electrons will be a maximum. This 'phase bunching' of electrons is maintained in a particular region of space and constitutes a sheet of transverse current to which each electron contributes as it passes through the resonance region. It is this current sheet that radiates the wave that bunches the electrons.

In terms of the picture just described we can now understand the mechanism of amplitude limiting. Assuming that the range of parallel velocities of the resonant electrons does not change appreciably with wave amplitude, we see that the peak value of the current within the interaction region is independent of the wave amplitude. Thus, if the wave amplitude should increase beyond the optimum value, the physical length of the spatial current pulse would be reduced, but its peak amplitude would not be increased; hence, the effective transverse current would be reduced. This process limits the wave amplitude.

To find the maximum length of the current pulse, we consider the variation in

resonance condition along the path. It is clear that the length of the resonance region must be maximized in order to maximize the effective sheet current. It is postulated that this condition obtains when the spatial variation of electron gyrofrequency and the Doppler-shifted wave frequency are matched. That is to say, the particles bunched by the output wave will radiate at a frequency determined by the change in gyrofrequency with distance and also by the change in the pitch angle of the particles. It is also clear that, if this interaction region is too long, the particles cannot remain in phase with the coexisting wave, and hence the bunching action will be lost. This limitation places a maximum value on the interaction region length. Thus, there is a length (~1000 km) of the current pulse that provides the maximum total sheet current, and, for lengths greater or less than ~1000 km, the total sheet current is reduced. This reduction explains the constant amplitude of the oscillator.

The frequency change with time can be derived with the aid of Figure 13. Here electrons resonating with waves of frequency f_1 move to the right with their streaming velocity, $v_\parallel$. As the electrons move they become bunched, and, at a distance dS down the field line, they radiate waves of frequency f_2. The waves of frequency f_2 propagate back to the starting point at their group velocity and resonate with a new group of electrons, which then repeat the process. By considering Figure 13 and the resonance conditions shown in Figure 11*a*, we can see that the change of frequency with time will depend upon the change of gyrofrequency with distance, the group velocity of the wave, the parallel velocity of the electrons, the ratio of the gyrofrequency to the wave frequency, and the pitch angle α of the electrons. The important point is that the frequency is a function of position with respect to the geomagnetic equator. It is now clear that, if the inter-

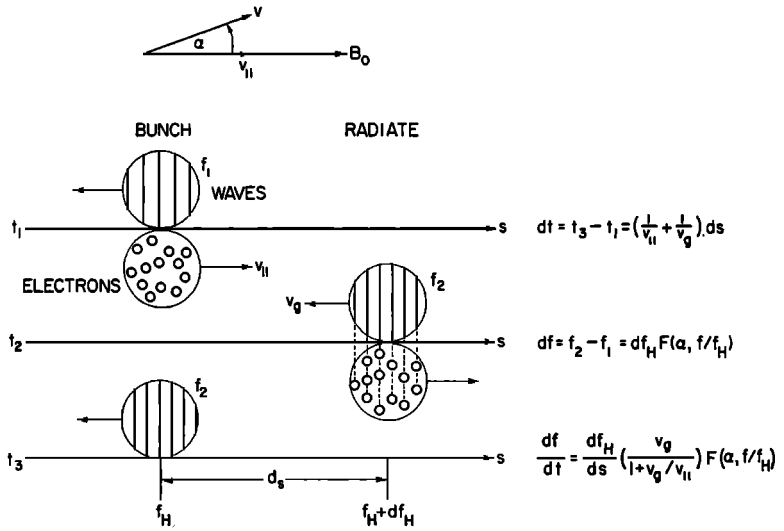

Fig. 13. Frequency change mechanism: Electrons spiral to the right at streaming velocity $v_\parallel$; generated waves propagate to left at group velocity v_g, α = pitch angle of electrons.

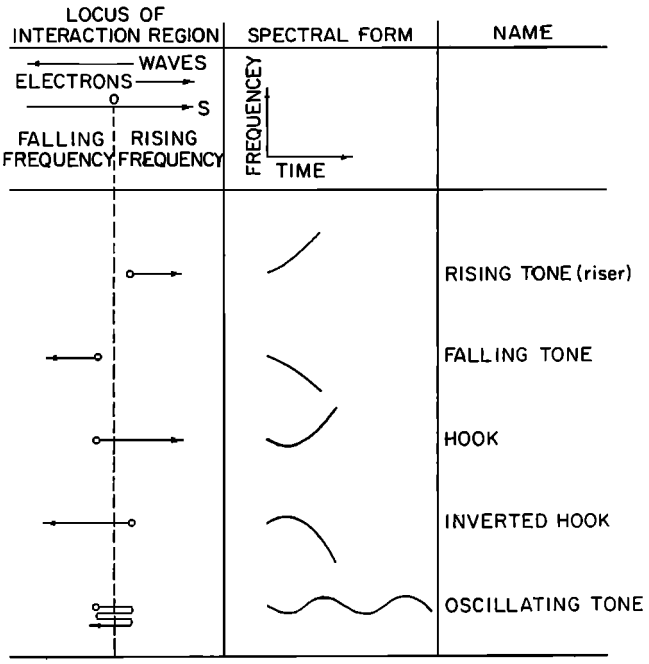

Fig. 14. Schematic diagram showing relation between the locus of the interaction region and the spectral form of the emission [after *Helliwell*, 1967].

action region is on the downstream side of the equator, the change of frequency with time will be positive, and, if it is on the upstream side of the equator, the frequency change will be negative. If the resonant particle flux is either greater or less than that required for equilibrium at a fixed location, the interaction region will drift, respectively, downstream (with the particles) or upstream (with the waves). The process of frequency change with time is illustrated in more detail in Figure 14. Here several initial positions and drifts of the interaction region have been assumed, and the corresponding frequency versus time curves have been sketched.

Emissions may be triggered by another signal that serves to provide the initial phase bunching required to start the oscillator. Emissions also can start spontaneously, and it is postulated that in this case the initial growth is the result of a small signal instability [*Kennel and Petschek*, 1966]. As we have already demonstrated, the feedback process, which is essential to explaining these emissions, would be maximized at half the gyrofrequency, where the ray directions show minimum spread. Thus, we have a natural explanation for onset of discrete emissions at half the gyrofrequency.

Termination of an emission is not as clearly understood but may depend upon the change in particle parameters with frequency. Also wave damping of the cyclotron or Landau type will tend to increase as the frequency rises, and this tendency may be a cause of the cutoff of rising emissions. In the case of falling

tone emissions, the resonance condition given in Figure 11*a* shows that, as the frequency decreases, it is possible for the parallel velocity of the resonant electrons to increase (assuming small changes in v_p); hence, the concentration of such electrons would be expected to decrease, thus reducing the flux of resonant particles.

Finally we must account for the triggering delay observed in the case of ASE's. It is clear from the process already described that it takes time to bunch the electrons and that the beginning of an oscillation requires the passage of about one bunching period. To the bunching period must be added the time required for the resulting radiation to reach the bunching region. This total time is between 50 and 100 msec, thus accounting for the triggering delay. Similarly the absence of triggering by Morse-code dots is explained by the fact that the dot does not last long enough to produce a self-sustaining current sheet.

In the mechanisms outlined above, generation of VLF emissions depends upon both the cold plasma properties that affect wave propagation and the resonant energetic particles that affect the growth process. Thus, it may be possible to employ VLF emissions in the study of both the thermal plasma and the energetic particle fluxes. Triggering of nonducted VLF emissions using a whistler-mode transmitter in a satellite could provide new data on the interaction process. Thus, the changes in the pitch angles of the interacting particles could be detected on the satellite from which the waves were transmitted. An experiment of this type has this advantage: the satellite can be located far from the interaction region, thus increasing the volume of space accessible to study from a single satellite.

SUMMARY AND CONCLUSIONS

Let us now briefly review the results described in previous sections and indicate some unsolved problems. For this purpose it is convenient to have a frame of reference that unifies the various phenomena presented; hence we shall employ the meridional plane representation of the magnetosphere shown in Figure 15, including compression by the solar wind [*Williams and Mead*, 1965]. The dayside has been selected because there is little evidence of low-frequency wave activity beyond the plasmapause at night. Within the plasmasphere, wave activity is relatively high both day and night.

The plasmapause is shown at $L = 4$, a position characteristic of mild magnetic disturbance ($K_p = 2 - 4$), and the boundary of the closed field lines lies between the lines marked 80° and 85.° Some typical whistler ducts are indicated. Regions of generation of VLF waves are shown dotted. The disk-shaped region in the equatorial plane is the origin of discrete emissions and associated hiss. From the observational data we know that emissions tend to be generated at all locations in this plane, with the possible exception of some areas in the tail of the magnetosphere. Emissions are observed out to latitudes of at least ±50°. It is supposed that nonducted discrete emissions from the equatorial plane are generally reflected at the LHR, as illustrated by the path beginning at $L = 6$; their observation by polar-orbiting satellites would then depend on whether the local LHR frequency were lower than the emission frequency.

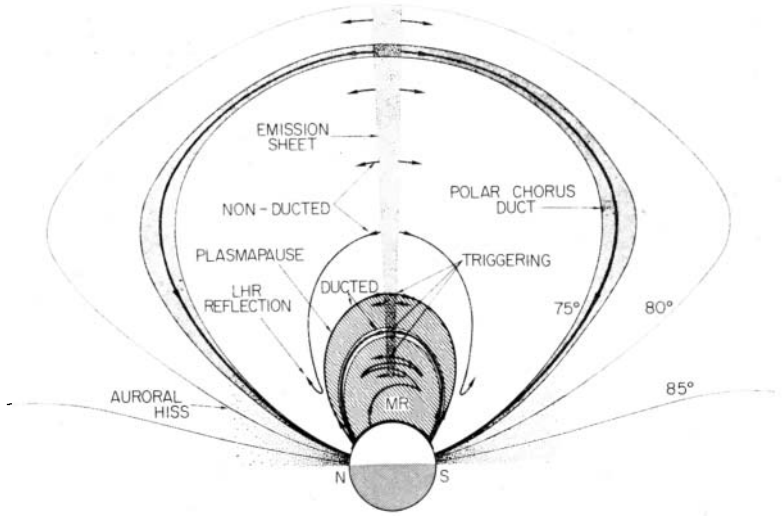

Fig. 15. Distribution of low-frequency waves in the geomagnetic meridional plane on the dayside of the earth.

The 'polar chorus duct' is intended to represent the prevalence of field-aligned enhancements of ionization observed in the auroral zone. It is supposed that some of these extend up to the equatorial plane and conduct the radiation down to the ground, where it is observed as polar chorus. MR whistlers within the plasmasphere are illustrated, including their tendency to produce wavegrowth and emissions in the equatorial plane as a result of Landau growth. Whistler ducts are shown at $L = 3$ and $L = 4$ and are excited by lightning impulses and man-made transmissions from the ground. Discrete emissions both spontaneous and triggered are common in ducts within the plasmasphere. Outside the plasmasphere spontaneous discrete emissions dominate.

The boundary of the plasmasphere is an especially active region for both wave propagation and emission. This may result in part from the unusually good trapping properties of the plasmasphere knee but also may be connected with enhanced energetic particle activity at the knee. In the auroral zones, a source of radiation is suggested by the dots, but very little is known about the location of the region of generation. We know that various kinds of noise can be seen throughout the polar regions including the polar cap, and the variety is such that much more research, using detailed spectrum analysis, is required to properly classify and study these phenomena. For example, we do not fully understand why there is very little correlation between the auroral hiss observed on the ground and the noise seen in satellites. Furthermore, there appear to be noise phenomena in the auroral zone that are seen only with electric antennas, indicating the possibility that some of the noise may be electrostatic. In any study of magnetospheric emissions simultaneous data on energetic particles are needed to test theories that have been proposed and to develop new ideas regarding the relationships between waves and particles.

Although we have learned much about the propagation of low-frequency waves in the magnetosphere, there is still much to be learned, including the discovery of new phenomena. One of the reasons for emphasizing continued research on low-frequency wave propagation is that the understanding of wave-particle interactions depends vitally on a clear picture of the related propagation factors.

In the last ten years the study of low-frequency waves in the magnetosphere has brought forth a bewildering variety of phenomena, many of which are now understood. This understanding has led to new tools for the study of the magnetosphere and has made valuable contributions to plasma physics. In the future we can expect that study of low-frequency waves in the magnetosphere will continue to provide new insights into the physics of the magnetosphere and the physics of plasma in general. The principal problem is not whether there are sufficiently interesting problems to tackle in the future, but which ones to tackle first.

Acknowledgments. This research was supported by the Air Force Office of Scientific Research under grant AFOSR-783-67A and by the National Aeronautics and Space Administration under grant NsG 174-SC/05-020-008. Data have been acquired through grants from the Atmospheric Sciences Section and the Office of Antarctic Programs of the National Science Foundation.

REFERENCES

Angerami, J. J., and D. L. Carpenter, Whistler studies of the plasmapause in the magnetosphere, 2, Electron density and total tube content near the knee in magnetospheric ionization, *J. Geophys. Res., 71,* 711, 1966.

Barrington, R. E., Some satellite observations of VLF resonances, *Proceedings of NATO Advanced Study Institute on Plasma Waves in Space and in the Laboratory, Roros, Norway, April 17–26, 1968,* in press, North Holland Publ. Co., Amsterdam, 1969.

Barrington, R. E., J. S. Belrose, and W. E. Mather, A helium whistler observed in the Canadian satellite Alouette 2, *Nature, 210,* 80, 1966.

Brice, N., An explanation of triggered VLF emissions, *J. Geophys. Res., 68,* 4626, 1963.

Brice, N., Fundamentals of very low-frequency emission generation mechanisms, *J. Geophys. Res., 69,* 4515, 1964.

Carpenter, D. L., Whistler studies of the plasmapause in the magnetosphere, 1, Temporal variations in the position of the knee and some evidence on plasma motions near the knee, *J. Geophys. Res., 71,* 693, 1966.

Carpenter, D. L., Ducted whistler-mode propagation in the magnetosphere: A half-gyrofrequency upper intensity cutoff and some associated wave-growth phenomena, *J. Geophys. Res., 73,* 2919, 1968*a*.

Carpenter, D. L., Recent research on the magnetospheric plasmapause, *Radio Sci., 3,* 719, 1968*b*.

Carpenter, D. L., N. Dunckel, and J. F. Walkup, A new VLF phenomenon: Whistlers trapped below the protonosphere, *J. Geophys. Res., 69,* 5009, 1964.

Gurnett, D. A., A satellite study of VLF hiss, *J. Geophys. Res., 71,* 5599, 1966.

Gurnett, D. A., and T. B. Burns, The low-frequency cutoff of ELF emissions, *J. Geophys. Res., 73,* 7437, 1968.

Gurnett, D. A., S. D. Shawhan, N. M. Brice, and R. L. Smith, Ion cyclotron whistlers, *J. Geophys. Res., 70,* 1665, 1965.

Guthart, H., T. L. Crystal, B. P. Ficklin, W. E. Blair, and T. J. Yung, Proton gyrofrequency band emissions observed aboard OGO 2, *J. Geophys. Res., 73,* 3592, 1968.

Helliwell, R. A., *Whistlers and Related Ionospheric Phenomena,* Stanford University Press, Stanford, California, 1965.

Helliwell, R. A., A theory of discrete VLF emissions from the magnetosphere, *J. Geophys. Res., 72,* 4773, 1967.

Heyborne, R. L., Observations of whistler-mode signals in the OGO satellites from VLF ground station transmitters, *SEL-66-094,* Radioscience Laboratory, Stanford Electronics Laboratories, Stanford University, Stanford, California, 1966.

Jørgensen, T. S., Interpretation of auroral hiss measured on OGO 2 and at Byrd Station in terms of incoherent Cerenkov radiation, *J. Geophys. Res., 73,* 1055, 1968.

Kennel, C. F., and H. E. Petschek, A limit on stably trapped particle fluxes, *J. Geophys. Res., 71,* 1, 1966.

Kimura, I., Effects of ions on whistler-mode ray tracing, *Radio Sci., 1,* 269, 1966.

Kimura, I., On observations and theories of the VLF emissions, *Planetary Space Sci., 15,* 1427, 1967.

Kimura, I., Triggering of VLF magnetospheric noise by a low-power (~100 watts) transmitter, *J. Geophys. Res., 73,* 445, 1968.

Liemohn, H. B., Radiation from electrons in a magnetoplasma, *Radio Sci., 69D,* 741, 1965.

Morozumi, H. M., Diurnal variation of auroral zone geophysical disturbances, *Rept. Ionosphere Space Res. Japan, 19,* 286, 1965.

Muzzio, J. L. R., Ion cutoff whistlers, *J. Geophys. Res., 73*(23), 7526–7529, 1968.

Smith, R. L., Propagation characteristics of whistlers trapped in field-aligned columns of enhanced ionization, *J. Geophys. Res., 66,* 3699, 1961.

Smith, R. L., An explanation of sub-protonospheric whistlers, *J. Geophys. Res., 69,* 5019, 1964.

Smith, R. L., and J. J. Angerami, Magnetospheric properties deduced from OGO 1 observations of ducted and nonducted whistlers, *J. Geophys. Res., 73,* 1, 1968.

Storey, L. R. O., An investigation of whistling atmospherics, *Phil. Trans. Roy. Soc. London, Ser. A, 246,* 113, 1953.

Storey, L. R. O., and J. C. Cerisier, Une interprétation des bandes de bruit au voisinage de la fréquence hybride basse observées au moyen le satellites artificiels, *Compt. Rend. Acad. Sci., Paris, 266,* 525, February 19, 1968.

Thorne, R. M., Unducted whistler evidence for a secondary peak in the electron energy spectrum near 10 kev, *J. Geophys. Res., 73,* 4895, 1968.

Williams, D. J., and G. D. Mead, Nightside magnetosphere configuration as obtained from trapped electrons at 1100 kilometers, *J. Geophys. Res., 70,* 3017, 1965.

Yabroff, I., Computation of whistler ray paths, *J. Res. NBS, D, 65D,* 485, 1961.